# Prediction of unsteady loading on a steam turbine blade

**By H. Kim†, H. Lee†, D. Kim‡, S. T. Bose‡ AND D. A. Philips‡**

A single rotor CFD model using wall-modeled Large Eddy Simulations (LES) was performed to predict the unsteady loading on the blade surface under partial admission. Geometry of the rotor blade of high pressure steam turbine of a 500 MW fossil-fuel power plant was used for this study. Periodically changing inlet boundary model was developed for single rotor model to simplify a full annular of the turbine. Single rotor model using LES showed a macroscopic pattern of excitation forces similar to the results of the two-stage full annular model using URANS (Unsteady Reynolds Averaged Navier-Stokes). Moreover, our LES model can capture the high-frequency fluctuation of forces on the blade. A corrected non-reflecting boundary condition was used to determine the amount of peak force around the border of the inactive arc.

## 1. Introduction

The control stage is the first stage in the entire turbine system; a stage consists of one stationary blade row and one rotating blade row. Typically it controls pressure and load of the entire turbine system during operation. When the turbine is under full admission, all control valves of the steam turbine are fully open (Valve-Wide Open condition, VWO) and the turbine generates its maximum power. Under partial admission, on the other hand, some valves are in a wide open mode and the other valves in a trim mode for part-load operation. Full admission (admission degree of $\epsilon = 1$) can show better performance when turbine is in full-load condition because the hot and pressurized steam is put through the nozzle box evenly. But under part-load conditions, full admission causes a huge throttling loss due to the partially closed valves. It decreases the turbine inlet pressure and overall efficiency of the power plant. On the other hand, partial admission closes one valve completely while the other three valves are fully opened ($\epsilon = 0.75$). With this sequential valve operation, power plant can reduce its power output while maintaining plant efficiency (Cotton 1993).

However, partial admission causes non-uniform flow at the first stage inlet. As shown in Figure 1, steam can only flow through the active arcs which are connected to open-valves. Non-uniformity gives unsteady loading that causes shock impact and vibrations to the first rotor blades. Unless this unsteady loading is incorporated into the design of the turbine, its structural reliability will be jeopardized. Thus, predicting the unsteady loading acting on the rotor blades of control stage is important in providing precise information for accurate mechanical and fatigue analysis.

Unsteady loading by partial admission has long been a subject of research. Ohlsson (1962) addressed an analytical approach using inviscid, incompressible model first. In the experiment by Lewis (2011)'s experiment on a four-stage turbine, the non-uniformity

† Doosan Heavy Industries and Construction, S. Korea
‡ Cascade Technologies Inc.

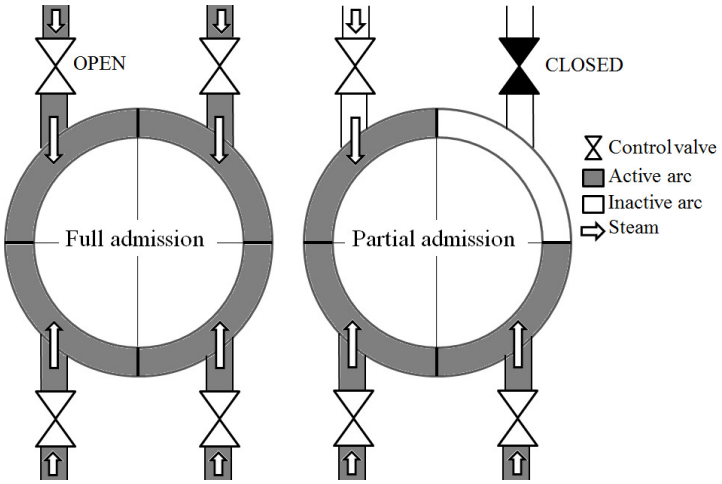


FIGURE 1. Operation concept of the control stage.

FIGURE 2. Computational domain of the two-stage full annular for conventional CFD of partial admission, arrow : flow direction.

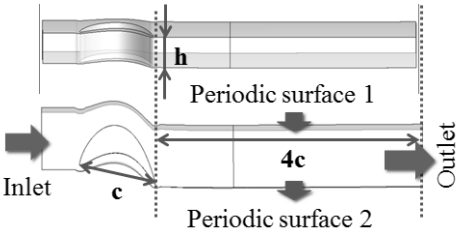


FIGURE 3. Computational domain of the single rotor model for LES, c = chord length of the control stage rotor blade, h = blade height.

in circumferential direction due to partial admission almost disappeared at the outlet of the second stage. Fridh (2012) addressed the characteristics of a 15% reaction turbine at various admission degrees ($\epsilon$) with a two-stage air turbine experiment. Sakai *et al.* (2014) compared quasi-three-dimensional CFD with experimental results and showed that a qualitative flow pattern of partial admission can be obtained via quasi-3D analysis. Recently, remarkable advancements of computational power have enabled two-stage 3-D CFD analysis for air turbine by Hushmandi (2010) and Kalkkuhl *et al.* (2014). Tokuyama *et al.* (2014) conducted a URANS CFD of a two-stage full annular supersonic turbine for a rocket turbo pump under partial admission. To the authors' knowledge, this study is the first attempt to apply LES to the analysis of partial admission of steam turbine. Conducting LES of a two-stage full annular model (FAM) at partial admission for industrial turbine design is very challenging. In this case, our turbine has 98 blades for the control stage and 188 blades for the second stage. Hence, were we to apply LES for two-stage FAM, literally hundreds of millions grid points would be required. As a first step in the application of LES in the steam turbine industry, a Single Rotor Model (SRM) for partial admission was developed to simplify the two-stage FAM in the present study.

## 2. Numerical modeling

A single Rotor Model (SRM) is part of the control stage. RANS calculation was conducted first to get whole flow information of the control stage (see Figure 2). Thereafter, boundary condition profiles for SRM were made from the RANS result.

Ansys CFX 15.0 with SST $k-\omega$ turbulence model is used for RANS calculation . For steady calculation, frozen rotor is chosen to interface type between stators and rotors, while transient rotor-stator type is used for unsteady analysis. Time step is $3.9 \times 10^6$ second, as same as revolution time over 4200. The number of mesh elements is 20 million. Total pressure and temperature are applied, which are 24 MPa and 863 K, respectively. Averaged outlet pressure is fixed to 17 MPa with radial equilibrium option.

Our SRM approach utilizes Wall-Modeled Large Eddy Simulation (WMLES) to predict unsteady loading precisely. The numerical solver used in this study is the CharLES, which is an explicit compressible flow solver for LES. CharLES solves spatially filtered compressible Navier-Stokes equations in conservative form based on a finite volume method. The equation of state and the speed of sound are defined using an ideal gas law (Bres *et al.* 2014). The code uses second order schemes in space, low numerical dissipation and a third-order Runge-Kutta scheme for explicit time advancement. To solve the sub-grid scale region, the Vremen model is used. On the blade surfaces, an equilibrium wall model is applied.

The main idea of the SRM is the periodically changing inlet profile, as shown in Figure 3. Inlet boundary conditions are simultaneously changed according to the accumulated simulation time. CharLES utilizes 7 property profiles for inlet boundary condition: axial velocity ($U_{ax}$), tangential velocity ($U_{th}$),radial velocity ($U_{rad}$), static pressure (p), temperature (T) and density ($\rho$) and turbulent kinetic energy (TKE).

Periodically changing profiles can be expressed by following function and added to CharLES using a hook file,

$$
\begin{aligned}
U_x &= U_{ax}, \\
U_y &= U_{th}\cos\theta + U_{rad}\sin\theta \\
U_z &= -U_{th}\sin\theta + U_{rad}\cos\theta \\
\phi(\theta, t) &= f(\theta + 120\pi t - 2\pi n)
\end{aligned}
$$

where $\phi$ is a property function, $\theta$ is the circumferential position (rad), $t$ is time (s) and $n$ is number of cycles.

Initial values(when t=0) for each inlet boundary conditions are extracted from steady RANS analysis of FAM (Figure 4).

Detailed boundary conditions for SRM-WMLES are as follows: rotating frame is used for global domain. Reynolds number based on the chord length, $c$ is $45.3 \times 10^6$ and the $Ma_{rel}$ based on the velocity viewed from the rotating frame is 0.4. The time step is determined by CFL number, 0.9. The averaged time steps are $5.0 \times 10^{-8}$ for the medium grid and $3.5 \times 10^{-8}$ for the fine grid. NSCBC (Poinsot & Lele 1992) is used for the boundary condition at outlet. Following arguments are used for specifying NSCBC condition. $p_{inf} = 18.208 \times 10^6$ Pa, $p_{relax}$ =0.1, $L_{ref}$ =0.5 and $T_{backflow}$ =815.5 K.

### 2.1. *Navier-Stokes characteristic boundary condition (NSCBC)*

Since the flow in the control stage is subsonic, NSCBC is used for the outlet boundary condition to eliminate the effect of the incoming wave. NSCBC may not be appropriate

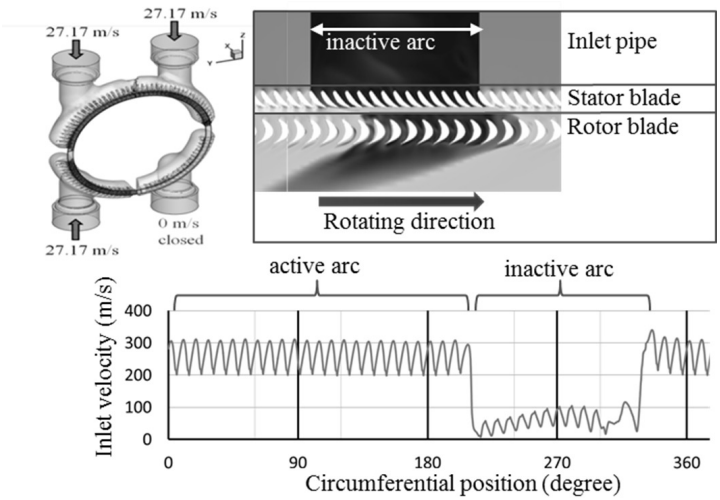


FIGURE 4. Periodically changing velocity profile produced by stator blade

because the real outlet is not at far downstream. Actually, there is the second stator behind the blade. As mentioned above, however, there are many limitations in applying exact physics because this analysis is a simplified case fitted to LES calculation. Thus, NSCBC seems to be a reasonable choice rather than pressure fixed condition or extrapolation.

The NSCBC approach uses the Navier-Stokes equations in their characteristic form where outgoing and incoming waves can be identified. The outgoing waves can be computed from interior cells. On the other hand, the incoming wave which comes from the outside of the domain must be treated properly. In NSCBC, the incoming wave amplitudes ($\pounds_1$) are imposed under the Local One-Dimensional Inviscid (LODI) Relation (Granet *et al.* 2010, Poinsot & Lele 1992). $\pounds_1$ is written as

$$\pounds_1 = K(p - p_t) \tag{2.1}$$

where K is the pressure relaxation coefficient and $p_t$ is the constant pressure at infinity. K is given by

$$K = \sigma c(1 - M^2)/l_{x1} \tag{2.2}$$

where, $\sigma$ is a constant varying from 0 (perfectly non-reflecting) to 0.25 (corrected non-reflecting), $c$ is the speed of sound, and $l_{x1}$ is a characteristic length of domain.

### 2.2. *Wall-model integration in an unstructured grid*

The work of Bodart & Larsson (2011) explains the details of the wall model. The model uses wall surface and associated surface where the flow field variables (e.g., u, T) are known from LES computation. It solves equilibrium boundary layer equations between these surfaces. The equations reduce to the coupled system of ODEs

$$\frac{d}{d\eta}\left(\left(\mu + \mu_{t,wm}\right)\frac{du_{||}}{d\eta}\right) = -S_m\left(\eta\right) \tag{2.3}$$

$$\frac{d}{d\eta}\left(\left(\mu + \mu_{t,wm}\right)u_{||}\frac{du_{||}}{d\eta} + \left(\lambda + \lambda_{t,wm}\right)\frac{dT}{d\eta}\right) = -S_e\left(\eta\right) \tag{2.4}$$

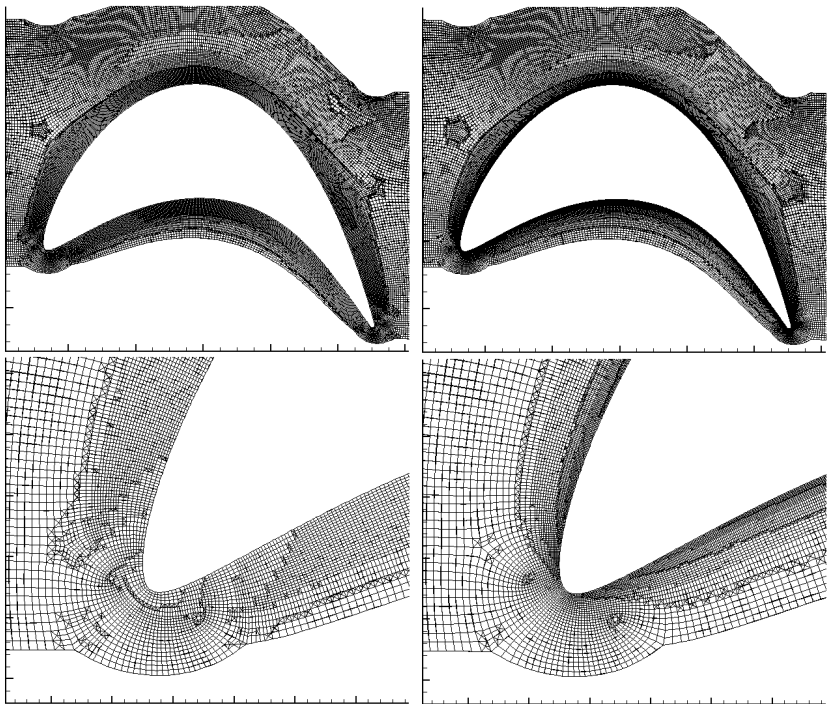

FIGURE 5. Grid resolution around blade (top) and leading edge (bottom) medium grid (left), fine grid (right)

where $\eta$ refers to the wall-normal coordinate, $u_{||}$ the wall-parallel velocity component, $\mu$ the dynamic viscosity, $\lambda$ the thermal conductivity, and $S_m$ and $S_e$ indicate the momentum and energy source terms, respectively. The eddy viscosity $\mu_{t,wm}$ and the turbulent thermal conductivity $\lambda_{t,wm}$ are written as

$$\mu_{t,wm} = \kappa\eta\sqrt{\rho\tau_\omega}\left[1 - exp\left(-\frac{\eta^+}{A^+}\right)\right]^2 \tag{2.5}$$

with $A^+ = 17$, $\kappa = 0.41$, $\lambda_{t,wm} = \mu_{t,wm}$, $C_p/Pr_{t,wm}$.

## 3. Results and discussion

Grid generation and the numerical studies were carried out. Figure 5 shows mesh density of a medium grid and a fine grid. The minimum edge length of the fine grid is 0.1 mm (0.09% of $C_l$, chord length) and the edge size of the medium grid is 0.25 mm. In order to demonstrate grid convergence, 3 cases with different grid refinement were tested. Figure 6 shows grid convergence by comparing the normalized tangential force ($f_t/f_{t,avg}$) and normalized axial force ($f_a/f_{t,avg}$) for each cases. The averaged tangential force ($f_{t,avg}$) is an averaged value within a stable active arc region. The medium grid and fine grid produced almost the same results.

In this study, an impulse turbine was used. The actual type of turbine can be categorized by its reaction. Reaction (R) is written as

$$R = \frac{\Delta h_{in-rotor}}{\Delta h_{in-stage}} = \frac{h_2 - h_3}{h_1 - h_3} \tag{3.1}$$

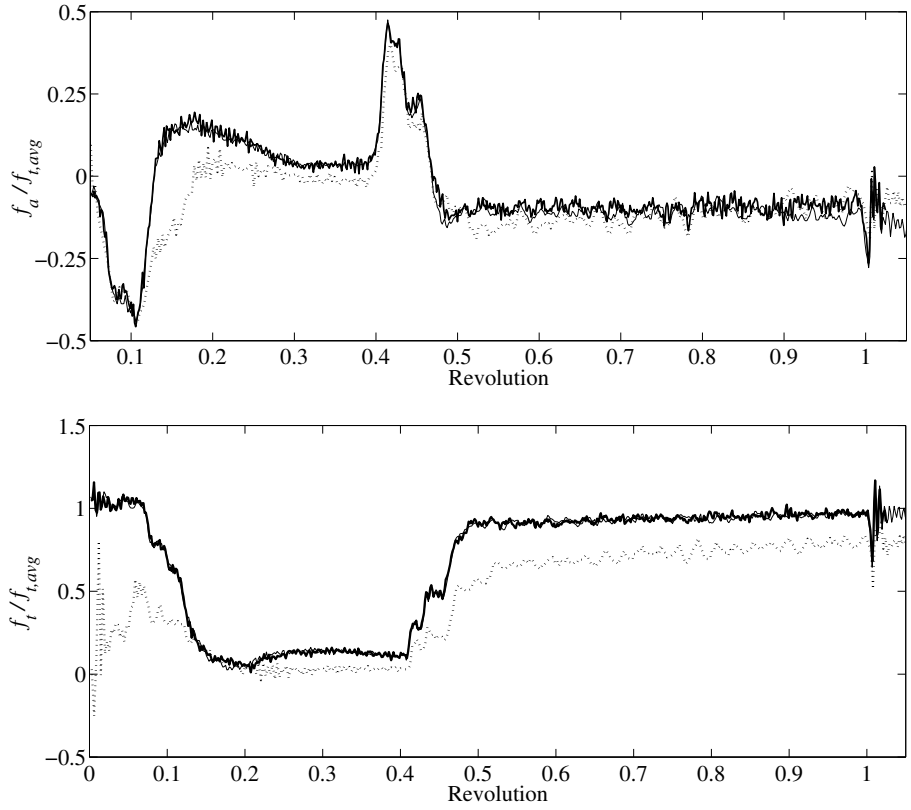


FIGURE 6. Grid convergence test, $f_t$ = tangential force acting on the blade, $f_{t,avg}$=averaged axial force within the active arc, coarse (dashed line), medium (bold line), fine (line)

In an isentropic process ($ds = 0$), the differential form of the enthalpy is represented by $dh = dp/\rho$. Then, the reaction can be written as

$$R \simeq \frac{p_2 - p_3}{p_1 - p_3} \tag{3.2}$$

where 1 is the stator inlet, 2 is the rotor inlet, 3 is the rotor outlet, $h$ is enthalpy change and $p$ is static pressure. It is a reaction turbine if $R = 0.5$, but it is and impulse turbine if $R = 0$. When $R = 0$, $p_2$ is equal to $p_3$, which means that the turbine inlet pressure is almost the same as outlet pressure and it is easy to cause adverse pressure gradient by partial admission. The outlet boundary condition should therefore be chosen with care.

The effect of outlet boundary conditions is displayed in Figure 7. Sponge and NSCBC are outlet boundary types of CharLES. Fixed static pressure is an outlet boundary type of Fluent, a commercial CFD tool. These cases conducted with same coarse mesh (200k). The result of a two-stage FAM (CFX, unsteady) was added as a reference result. As demonstrated in earlier research (e.g. Pigott 1980 and Hushmandi 2010), when a rotor enters an inactive arc, there will be a sudden peak of tangential force ($f_t$), followed by rapid drop in $f_t$. The sponge boundary condition could not predict the peak at all (see the inset in 7). $f_t$ calculated by Fluent is way below that of the two-stage FAM. In the Fluent case, influence of the downstream was too strong so that a reverse flow occurred

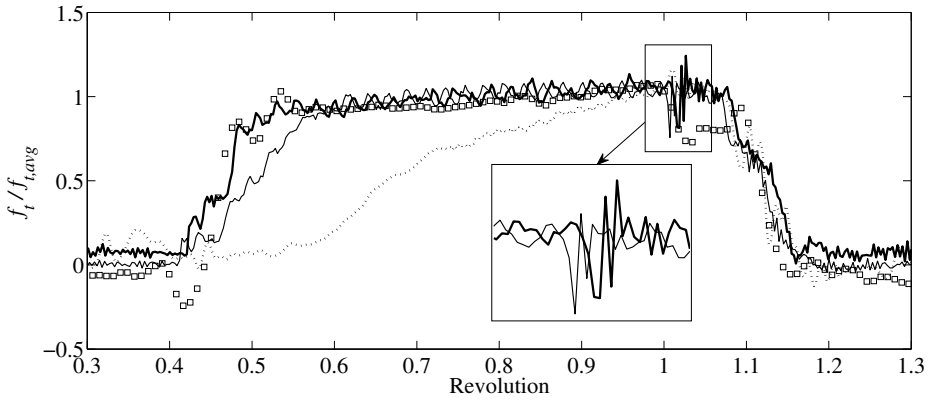


FIGURE 7. Effect of boundary condition at outlet, sponge (line), NSCBC (bold line), fixed pressure of Fluent (dashed line), two-stage FAM (square)

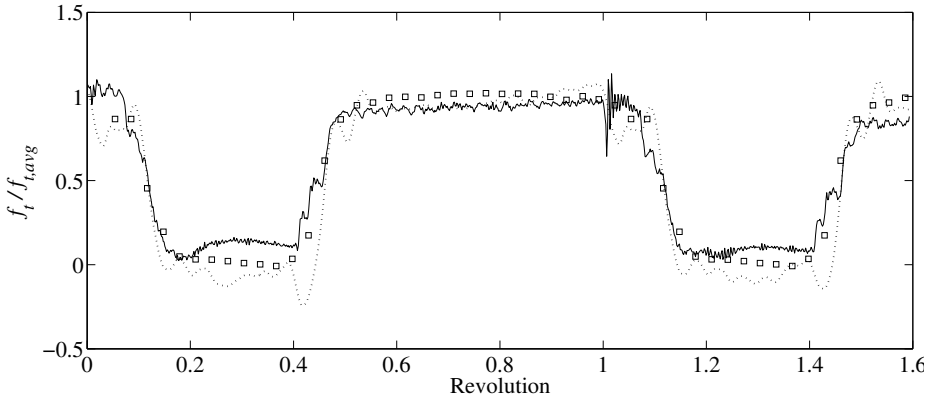


FIGURE 8. Unsteady loading acting on a rotor blade, SRM-LES (line), FAM-RANS-steady (square), FAM-RANS-unsteady (dashed line)

from the outlet. NSCBC was the best boundary condition for the single rotor model since it shows qualitatively similar flow patterns in comparison.

Figure 8 shows a typical force pattern in the control stage. When the control stage faces an inactive arc, the momentum of the fluid in the rotor channel becomes very low, causing a sudden drop in pressure drop on the suction side. This causes the tangential force to increase. The excitation force from SRM is well agreed to FAM-RANS steady and unsteady results, as presented in Figure 8. However, there is some disagreement about the boundary between active and inactive arc. That is possibly due to the assumption used in SRM. While FAM includes the control stage stator, the second stage and the cavity, SRM models the control stage rotor only. In the SRM, the transient inlet boundary condition models the wake flows from the first stage stators and the interface between the first stage and the second stage is replaced by the characteristic non-reflective outlet boundary condition, respectively. The modeled boundary conditions may cause the disagreement. In addition, the circumferential periodicity of SRM is an artifact - the actual blades experience circumferential variations as they moves around the arc. Especially, on the moment that the active arc ends, the periodicity of control stage is invalid; inactive flow

enters from both upside and downside of the domain, which does not occur in the real stage. Nevertheless, SRM-LES results show a peak in the excitation force in the boundary as well as reasonable agreement with FAM-RANS results. Although there are issues of SRM-LES that need to be dealt with in the future, the current study demonstrated the feasibility of applying LES in the control stage.

## 4. Conclusion and future work

The unsteady loading on the blade in the control stage is estimated by the compressible LES solver, CharLES, with an equilibrium wall model. The control stage case is simplified to the SRM using the transient inlet boundary condition and NSCBC. Computing the excitation forces on the control stage has been well known for its difficulty due to extremely high Reynolds number, stiff velocity variation (0 to 400m/s), and ultra-supercritical steam properties. Nevertheless, the wall-modeled LES was applied for the first time and produced lots of interesting results compared to unsteady RANS. It shows meaningful results in practical point of view, as follows. First of all, much fewer grid elements is used, compared to the two-stage FAM. Also, it is capable to capture high frequency force and small eddy that RANS cannot resolve. Finally, it can predict similar excitation forces on the blade in comparison with the two-stage FAM.

It is anticipated that the ultra-supercritical region and a full annulars model will be considered in forthcoming research. Finally, experiments at Doosan's turbine test facility will be performed in the near future to validate these LES results.

*Acknowledgments*

The authors would like to thank Prof. Moin and CTR members for their hospitality and technical support. The authors acknowledge use of computational resources from the Certainty cluster awarded by the National Science Foundation to the CTR.

## REFERENCES

Bodart, J. & Larsson, J. 2011 Wall-modeled large eddy simulation in complex geometries with application to high-lift devices. *Annual Research Briefs*. Center for Turbulence Research, Stanford University.

Bres, G., Bose, S., Ham, F., Kim, D., Le, H., Philips, D., Saghafian, A. & Shunn, L. 2014 *CTI User's & Developer's Manual*. Cascade Technologies Inc.

Cotton, K. 1993 *Evaluating and improving steam turbine performance*. Cotton Fact Inc.

Fridh, J. 2012 *Experimental investigation of perfrmance, flow interations and rotor forcing in axial partial admission turbine.* PhD thesis, KTH.

Granet, V., Vermorel, O., Leonard, T., Gicquel, L. & Poinsot, T. 2010 Comparison of nonreflecting outlet boundary conditions for compressible solvers on unstructured grids. *AIAA J.* **48**, 2348–2364.

Hushmandi, N. B. 2010 *Numerical analysis of partial admission in axial turbines.* PhD thesis, KTH.

Kalkkuhl, T. J., Engelmann, D., Harbecke, U. & Mainach, R. 2014 Numerical analysis of partial admission flow in an industrical steam turbine. *Proc. ASME Turbo Expo 2014*. GT-2014-26774.

Lewis, K. 2011 The influence of partial admission on the performance of a multistage turbine. *Internal Report*, Cambridge University, UK: Whittle laboratory.

Ohlsson, G. 1962 Partial-admission turbine. *J. Aerospace Sci.* **29**, 1017–1028.

Pigott, R. 1980 Turbine blade vibration due to partial admission. *Int. J. Mech. Sci.* **22**, 247–264.

Poinsot, T. & Lele, S. 1992 Boundary conditions for direct simulations of compressible viscous flows. *J. Comput. Phys.* **101**, 104–129.

Sakai, N., Harada, T. & Imai, Y. 2014 Numerical estimation of the unsteady force on rotor blades in a partial arc admission stage of an axial turbine. *Proc. ASME Turbo Expo 2014*. GT-2014-26774.

Tokuyama, Y., ichi Funazaki, K., Kato, H., Shimiya, N. & amd Masaharu Uchiumi, M. S. 2014 Computational analysis of unsteady flow in a partial admission supersonic turbine stage. *Proc. ASME Turbo Expo 2014* GT2014-26071.